Nuclear Inst. and Methods in Physics Research B 440 (2019) 101–106

Contents lists available at ScienceDirect

Nuclear Inst. and Methods in Physics Research B

journal homepage: www.elsevier.com/locate/nimb

Structural and optical studies of gamma irradiated N-doped 4H-SiC

Indudhar Panduranga Vali[a], Pramoda Kumara Shetty[a,*], M.G. Mahesha[a], V.G. Sathe[b], D.M. Phase[b], R.J. Choudhary[b]

[a] Department of Physics, Manipal Institute of Technology, Manipal Academy of Higher Education, Manipal 576104, India
[b] UGC-DAE Consortium for Scientific Research, University Campus, Khandwa Road, Indore 452017, India

ARTICLE INFO

Keywords:
Silicon carbide
Gamma irradiation
LOPC modes
PL
XRD

ABSTRACT

In this paper, the gamma irradiation effects on the structural and optical properties of N-doped 4H-SiC (n-4H-SiC) is presented up to a cumulative gamma radiation dose of 1500 kGy. The studies showed marginal and inconsistent variation in the *c*- and *a*-axis lattice constants of 4H-SiC due to the accumulation of gamma-induced defect states. The modifications in the longitudinal optical plasmon-phonon coupled (LOPC) modes, Biedermann absorption bands, Urbach energy (E_U) and defect related photoluminescence (DPL) bands are discussed at different (500, 1000 and 1500 kGy) irradiation doses. Despite these effects, the overall gamma-induced disorder ($1 - A_{norm}$) and variation in the free carrier concentrations (n) are found to be negligible and demonstrating the radiation resistant property of n-4H-SiC under gamma radiation environment.

1. Introduction

Silicon carbide (SiC) is a well-known semiconductor material since three decades. The properties of SiC are found to depend on the stacking sequence of the Si-C bilayers i.e., polytypism or one-dimensional polymorphism. So far more than 200 polytypes of SiC have been identified. However, the polytypes such as 3C-SiC, 4H-SiC and 6H-SiC have remained most popular because of their practical importance and stability [1]. Over the last three decades, extensive research on these polytypes have contributed greatly to their commercialization in the form of single crystal wafers. Among these, 4H-SiC polytype is considered as most desirable candidate for device applications due to its superior properties such as wide band gap and isotropic electron mobility [1,2]. The doping of nitrogen (N) impurities into 4H-SiC crystal gives the material n-type conductivity. Commercially, the N-doping into 4H-SiC is carried out by means of ion implantation technique. Due to this reason 4H-SiC is one of the leading material for the most practical products including Schottky-barrier diodes (SBDs), metal-oxide semiconductor field-effect-transistors (MOSFETs), and junction field-effect-transistors (JFETs) [1–4].

Due to superior physical properties of 4H-SiC, it has been also proposed for so called radiation-hard devices. With the development of space technology and nuclear industry, the 4H-SiC based devices would be used for working in the aerospace, aviation, and reactor fields. As a result, the devices are commonly exposed to both particles and electromagnetic radiation. Therefore, scrutiny of the irradiation-induced effects on 4H-SiC is crucial to predict on the behavior of device properties [5,6]. In the last two decades, various researchers have performed electron irradiation [7–10] proton irradiation [10,11], neutron irradiation [12,13] and ion irradiation studies [14–19] to account for the intrinsic as well as irradiation-induced defect states in 4H-SiC. In particular the ion or neutron irradiation at higher irradiation doses greatly disturbs the periodic arrangement of atoms of the 4H-SiC crystal lattice due to the accumulation of defect states and defect cascades. This leading to noticeable radiation damage in the material. Apart from characterizing the defect states, the radiation damage can be also accounted by describing the evolution of different irradiation-induced spectral signatures in the optical absorption spectra, Raman scattering spectra and Rutherford back scattering spectra [16–19]. Despite considerable interest in carrying out these studies on 4H-SiC after exposing it to the highly damaging radiations like heavy ions and neutrons, it is also interesting to extend the similar studies for lower damaging radiations like electrons and gamma rays. Such studies would play crucial role in the better understanding of the substrate contribution on the device properties. In this view the present article reports on the gamma-induced (Co-60) modifications in the structural and optical properties of n-type 4H-SiC. The studies are presented systematically by using different characterization techniques and the underlying mechanisms are discussed. Also a plausible explanation on the role of gamma-induced effects observed in the present study is discussed with the some of the available reports on the device properties (p-n junction diode, Schottky diode and MOSFETs) which are exposed to gamma irradiation at higher irradiation doses.

* Corresponding author.
E-mail address: pramod.shetty@manipal.edu (P.K. Shetty).

https://doi.org/10.1016/j.nimb.2018.12.016
Received 4 October 2018; Received in revised form 5 December 2018; Accepted 6 December 2018
Available online 14 December 2018
0168-583X/

2. Experimental details

The N-doped 4H-SiC (0001) polished wafers (n-4H-SiC) having resistivity in the range 0.012–0.030 Ω.cm and thickness of 330 ± 25 µm were procured from Semiconductor Wafer, Inc. (Taiwan). The wafer is diced in square pieces of dimension 0.5 × 0.5 cm and cleaned according to the procedure described in Ref. [20]. The cleaned samples are subjected to gamma irradiation using Gamma Chamber GC-5000 situated at Indira Gandhi Centre for Atomic Research (IGCAR), Kalpakkam India. The Gamma Chamber GC-5000 has a compact and shielded ^{60}Co gamma irradiator with controlled modes of operation. It consists of 8 ^{60}Co pencil sources arranged in annular manner around the irradiation volume. The diameter and cylindrical height of the chamber was 17.2 cm and 20.5 cm respectively. The ^{60}Co source emits gamma photons of two different energies 1.17 and 1.33 MeV. The strength of the ^{60}Co source during the irradiation experiment was approximately 2.8 kGy/h (~78 rad/s) [20]. The samples are irradiated up to a cumulative radiation dose of 1500 kGy. The time took for delivering 1500 kGy dose on to the samples was about 535.7 h (~22.5 days). The X-ray diffraction (XRD) patterns, and Raman scattering (RS), UV–Visible absorption and photoluminescence (PL) spectra are measured at 500, 1000 and 1500 kGy irradiation doses.

The XRD studies are carried out by using Bruker D8 Advance which is operating at 40 kV and 40 mA (Cu-Kα, λ = 1.5406 Å). The Raman scattering spectra of n-4H-SiC were recorded at room temperature in a back scattering symmetry using a Jobin Yvon Horibra LABRAM-HR visible spectrometer. The spectra are obtained by exciting the samples with 473 nm line of an Ar^+ laser which was focused on a 1 × 1 µm^2 spot. The UV–Visible absorption spectra were taken in the wavelength range of 350–800 nm using Shimadzu UV − 1800 spectrophotometer. The PL spectra in the wavelength range of 350–620 nm is measured at 325 nm excitation by using Horiba Jobin Yvon 450 W Illuminator.

3. Results and discussion

3.1. XRD analysis

According to the extinction rules determining the crystal symmetry, the hexagonal structured 4H-SiC with space group $P6_3mc$ will show diffraction peaks from (000l) planes, where $l = 2n$ (n is an integer) [21,22]. The XRD peaks corresponding to $l = 4$ (or$n = 2$) and $l = 8$ (or$n = 4$) are shown in Fig. 1(a). Before irradiation, the (0004) and (0008) peaks are observed at $2\theta = 35.66$Â° and $2\theta = 75.40$Â° respectively. But after irradiation marginal shift in the peak position, variation in the peak intensity and peak width are observed with respect to the unirradiated sample. These modifications are mainly attributed to the presence of gamma-induced defect states in n-4H-SiC. No radiation-induced peaks are observed in the 2θ range of $20 - 80$Â°. The c- and a-axis lattice constants of 4H-SiC are determined before and after gamma irradiation by using the following relations [23]:

$$c = \frac{\lambda \bullet l}{2\sin\theta_{00l}} \tag{1}$$

$$a = \lambda \bullet h' \sqrt{\left(\frac{1}{3\left[\sin\theta^2_{h'0l'} - \left(\left(\frac{l'}{l}\right)^2 \sin\theta^2_{00l}\right)\right]}\right)} \tag{2}$$

where $\lambda = 1.5402$Å. Here, the c-axis lattice constant is determined from (0004) and (0008) peaks, and a-axis lattice constant is determined from $(10\bar{1}4)$ peak which is observed at $2\theta = 48.20$Â° for the unirradiated sample. The evaluated values for the unirradiated samples are found to agree with the other literatures [23]. The variation of c- and a-axis lattice constants of 4H-SiC at different gamma irradiation doses is shown in Fig. 1 (b). As noticed, both the lattice constants are exhibiting

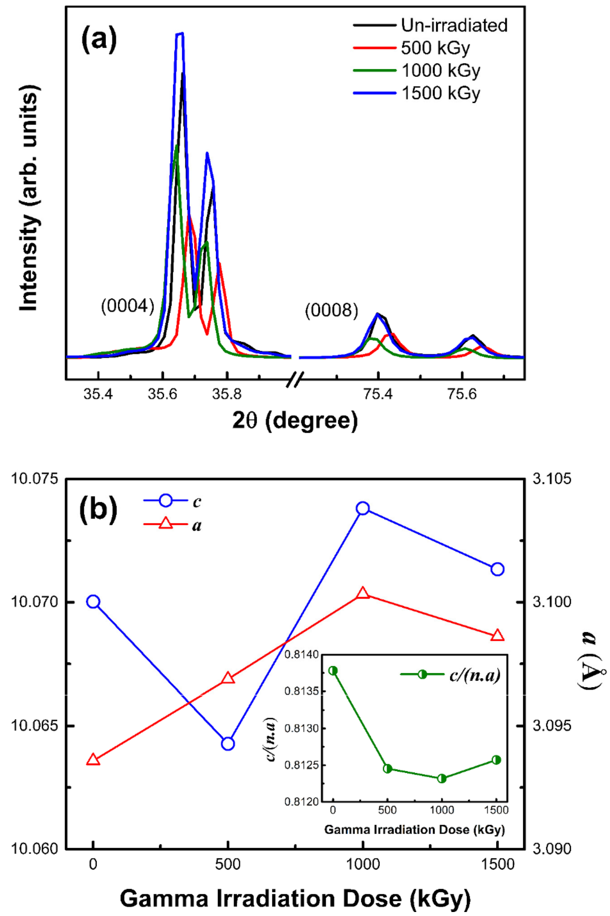

Fig. 1. (a) (0004) and (0008) reflections of 4H-SiC before and after gamma irradiation (b) variation of c-axis and a-axis lattice constants of 4H-SiC at different gamma irradiation doses. Inset shows the variation of $c/n.a$ ratio at different gamma irradiation doses.

small but irregular variations at different gamma irradiation doses. This indicates that due to the anomalies in the accumulation of defect states at both hexagonal (h) and cubic (k) sites of the crystal (site effect) the lattice distortion along c- and a-axis directions of the 4H-SiC crystal are different. Therefore by determining $c/(n.\ a)$ ratio the overall distortion in the bonding tetrahedral of the crystal lattice can be estimated. Since $c/(n.\ a)$ ratio represents the significant criterion for the hexagonal (h) and cubic (k) proportion of the Si-C bilayer stacking sequences and any deviation from its initial value is an indicative of the modified nature of the bonding tetrahedral of the crystal lattice (here n is equal to 4 for 4H-SiC polytype) [1,2,23]. The decrease in the $c/(n.\ a)$ ratio for all irradiated samples as noticed from the Fig. 1 (b) inset is clearly attributed to gamma-induced distortion in the bonding tetrahedral of the crystal lattice by generating the various defect states at both h- and k-sites of the 4H-SiC crystal. On an atomic scale this causes an anisotropy in the lattice deformation (either contraction and/or dilation) along the three crystallographic directions of 4H-SiC. Due to this reason we have noticed anomalies in the peak shift with respect to the unirradiated sample.

3.2. UV–Visible absorption spectra analysis

The optical absorption spectra in 4H-SiC or any other semiconductors are normally dominated by transitions from the valence to the conduction bands. But the spectra can also show relatively strong defect related absorption bands below the fundamental gap. Therefore, the optical absorption data give access to energy band gap (E_g) and

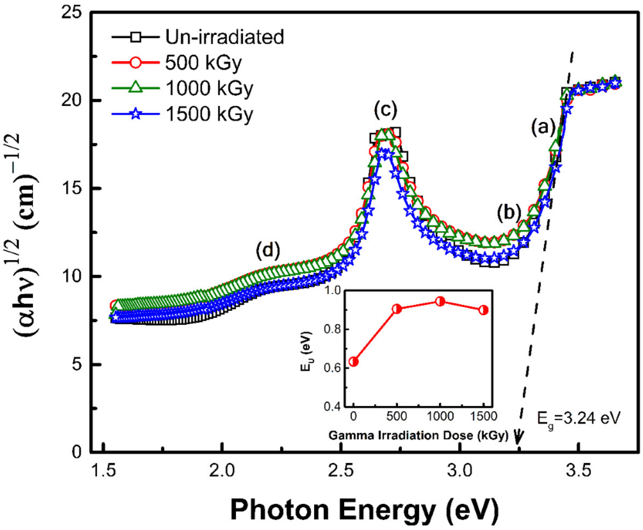

Fig. 2. Absorption spectra of n-4H-SiC before and after gamma irradiation. Inset plot shows the variation of Urbach energy (E_U) determined in the region 3.20–3.24 eV at different gamma irradiation doses.

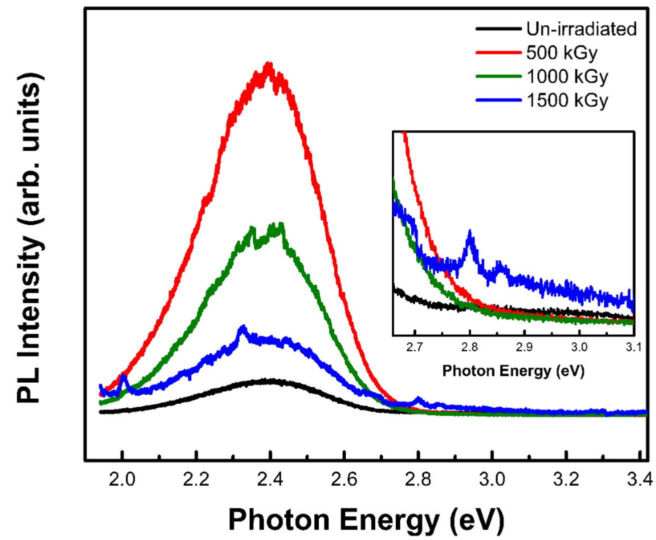

Fig. 3. Room temperature photoluminescence (RTPL) spectra of n-4H-SiC before and after gamma irradiation. Inset shows the enlarged PL band observed in the energy range 2.7–3.0 eV.

band gap disorder i.e., Urbach energies (E_U) [17,24]. In the Fig. 2 the optical absorption spectra of n-4H-SiC are shown before and after gamma irradiation at different irradiation doses. The four characteristic features as marked are the representative of band to band (a), band to donor level (b), free electron absorption into higher conduction bands (c) also known as Biedermann absorption bands, and absorption bands from the defect states (d) [25,26].

The absorption bands (a) is the region where the band-to-band absorption sets in. By fitting Tauc's equation [27] for an indirect allowed transitions in the region (a), E_g of 4H-SiC is found to be 3.24 eV. No noticeable modification of E_g is observed after gamma irradiation. However just below the Tauc region (in the region (b)) we notice some modifications in the exponential form of the energy dependence on absorption i.e., the electronic transitions from localized states in the band tails to the extended states (Urbach tail). This clearly indicates band gap disorder and it is usually estimated by determining the Urbach energy (E_U) by fitting the following relation [17,28]:

$$\alpha \approx \alpha_0 \exp\left(\frac{h\nu}{E_U}\right) \tag{3}$$

where α is absorption co-efficient, α_0 a proportionality constant and $h\nu$ photon energy. We determined E_U in the region of 3.20 to 3.24 eV and its variation at different irradiation doses is shown in the inset of Fig. 2. As noticed, after gamma irradiation the value of E_U is increasing. This is clearly an indicative of increase in the band gap disorder caused due to the fluctuations in the dopant energy levels, accumulated defect states in the band gap, and distortion in bond angles and/or bond length. Similar observations are also reported for ion irradiated 4H-SiC [17,19].

3.3. PL spectra analysis

The PL spectra of n-4H-SiC is quite complex due to the substitution of N-impurity as well as point defects at certain nonequivalent sites (*h*-and *k*-sites) of the 4H-SiC crystal [29]. Most of the PL studies of n-4H-SiC reports on the E_A (alphabet lines) [7,14,30] D_I [31,32] and D_{II} [33,34] PL defect bands which are observed at low temperature. These PL bands are explained in terms of complicated defect centers including di-vacancies, di-interstitials, tri-interstitials, split interstitials or other defect complexes. But only few native defects, namely, the carbon and silicon vacancies (V_C and V_{Si}) are actually recognized from the experiments [35].

The PL spectra of n-4H-SiC before and after gamma irradiation is shown in Fig. 3. The broad PL band peaked around 2.4 eV is present in both unirradiated and irradiated samples. This band is the signature of n-4H-SiC and it is broadly known as defect related photoluminescence (DPL) [36]. It is attributed for the presence of PL signals from the various recombination centers upon N-doping. These bands are similar to the defect related absorption bands (d) as shown in Fig. 2. The main recombination path of DPL usually occurs via the donor-acceptor pairs (DAP). The DPL band is attributed for some sort of defect complexes involving C-atoms and N-atoms which are bonded to point defects. [36]. As noticed, for the gamma irradiated samples DPL intensity has increased this suggesting an increase in the number of defect states. However, PL signal is greater for the 500 kGy irradiated sample compared to that of 1000 and 1500 kGy irradiated samples. This implies the fact that the defect concentration is comparatively greater at 500 kGy irradiation dose than at higher radiation doses. The decrease at higher irradiation doses could be due to the self-annealing properties of the gamma induced defect states or due to the occurrence of outward migration of the defect states in SiC [37]. However, the PL signals of the most stable defects states were found to be remained in the crystal. This is as noticed from the PL signals which are observed at ~2.0 and 2.8–2.9 eV (Fig. 3, inset). The PL signal at ~2.0 eV is attributed to carbon vacancies, while the bands in the range ~2.8 to 2.9 eV (which are well-known E_A PL bands at low temperature PL) are attributed for the carbon Frenkel pairs or carbon interstitials [7].

3.4. Raman spectra analysis

According to zone folding scheme, the dispersion curves of the phonons propagating along the (0001) direction in 4H-SiC crystal gives the folded modes at Γ point. Therefore, the phonon branches of 4H-SiC are known to be the folded transverse optical (FTO) and folded longitudinal optical (FLO) modes [38]. In the back scattering symmetry, the first order Raman spectra (FORS) of 4H-SiC consists of three phonon bands havingA_1, E_1 and E_2 symmetries. The phonon modes observed in the range 650–1350 cm^{-1} are shown in Fig. 4. Usually, theE_2(FTO), E_1(FTO) andA_1(FLO) modes of 4H-SiC are observed at777cm^{-1}, 797cm^{-1} and 964cm^{-1} respectively [18,38,39]. However, in the present case A_1(FLO) mode is exhibiting an asymmetric broadening up to 1250cm^{-1} due to plasmon-phonon coupling effect. Since 4H-SiC is a polar semiconductor which generates free carriers in the crystal as a result of N-doping and when these free carriers are excited by photons (now called

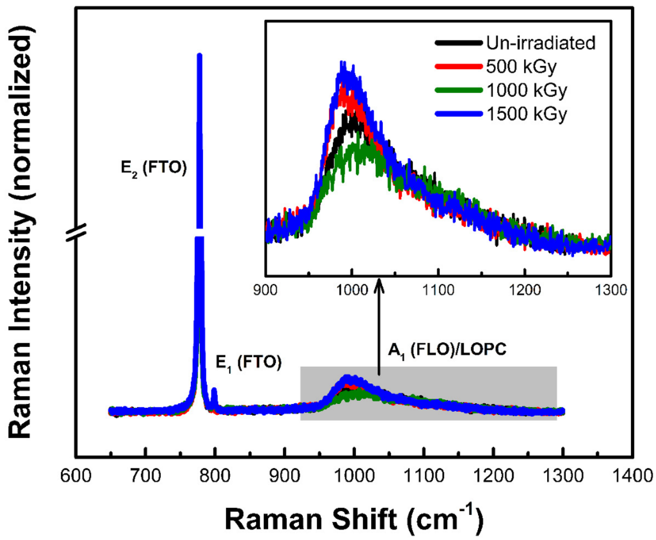

Fig. 4. First order Raman spectra of n-4H-SiC before and after gamma irradiation at different irradiation doses. The spectra is normalized to the E_2(FTO) mode of the un-irradiated n-4HSiC. The inset shows the enlarged LOPC mode.

as plasmons) couple strongly with lattice phonons due to their interaction via electric fields. This leading to a shift and asymmetric broadening of the A_1(FLO) mode. This resulting coupled mode is known as longitudinal optical phonon coupling (LOPC) mode (it is also observed in the other wide band gap semiconductors like GaN and GaAs) [38,40]. As noticed from Fig. 5, the LOPC mode is noticeably varying compared to E_2 (FTO) and E_1 (FTO) modes after gamma irradiation. Further, no additional bands are observed in the range of $100 - 1800\text{cm}^{-1}$.

To account for the overall gamma-induced disorder in the 4H-SiC crystal, the spectra is fitted by four Lorentz peaks as shown in Fig. 5. As noticed from the peak fitting parameters such as peak positions and peak widths (values given in bracket), the peak parameters of the LOPC mode are greatly varying compared to that of E_2(FTO) and E_1(FTO) modes. This indicates that LOPC mode is sensitive to the presence of gamma-induced defect states in n-4H-SiC. From the fitted spectra we estimated the total irradiation-induced disorder parameter ($1 - A_{norm}$) by using the following relation [16,18,41]:

$$1 - A_{\text{norm}} = 1 - \frac{A_{\text{Irradiated}}}{A_{\text{Un-irradiated}}} \tag{4}$$

where $A_{\text{Irradiated}}$ is total area of the Lorentz fitted lines of the irradiated sample spectra and $A_{\text{Un-irradiated}}$ is the total area of the Lorentz fitted lines of the un-irradiated sample. If the evaluated value is found to be greater than unity ($1 - A_{norm} > 1$) then it is an indicative of the irradiation-induced disorder in the crystal [16,18,41]. In the Fig. 6 the variation of $1 - A_{norm}$ is shown at different gamma irradiation doses. It is clearly noticed that the maximum gamma-induced disorder is observed at 1000 kGy dose compared to other irradiation doses. Similar observations are also quite evident from maximum shift in the XRD peak position, $c/(n.\ a)$ ratio (Fig. 1) and Urbach energies (insert, Fig. 2) compared to other irradiation doses. However, the maximum gamma-induced disorder at 1000 kGy is not greater than 10% (Fig. 6) and it is found to recover as the irradiation dose is increased to 1500 kGy. This could be due to the decrease in defect concentration via recombination processes (Fig. 3). The analogous features in the recovery of device

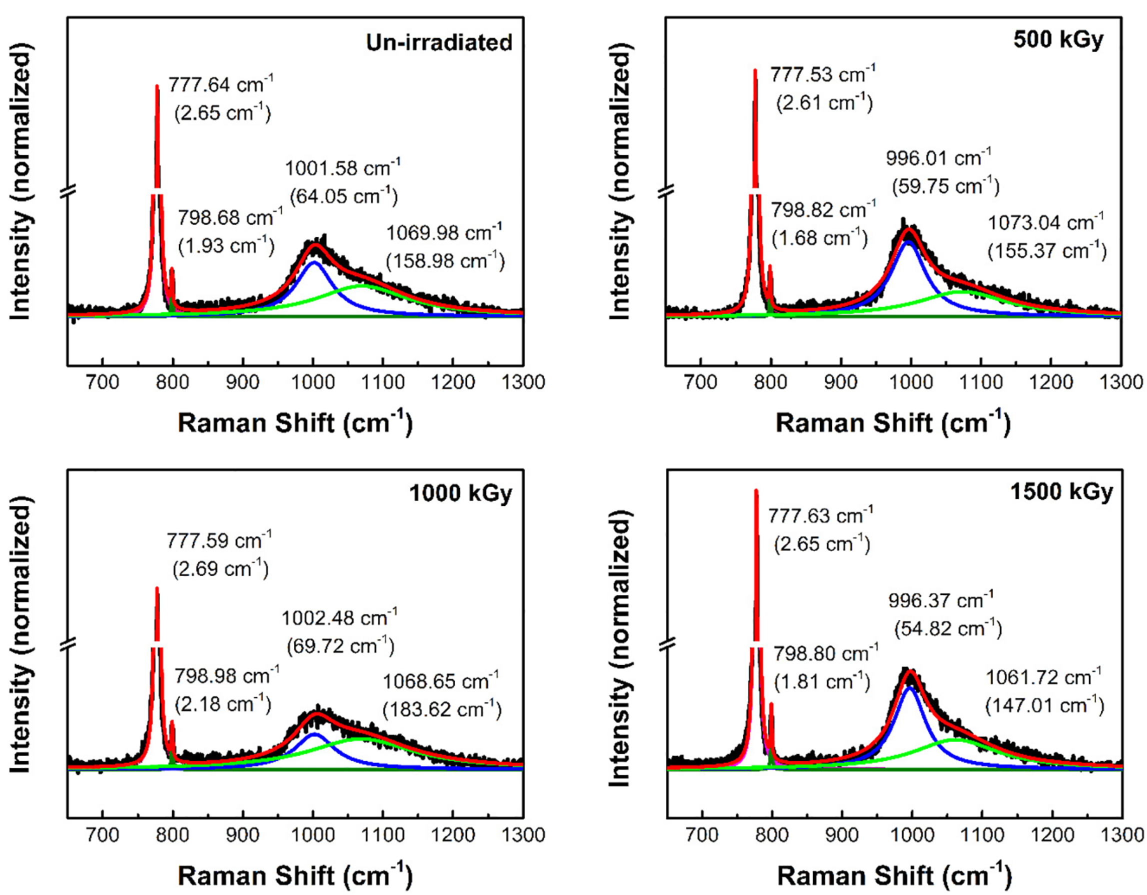

Fig. 5. First order Raman spectra of n-4H-SiC before and after gamma irradiation fitted by Lorentz peaks. The positions of the Raman modes are indicated by wave number and its width in the braces.

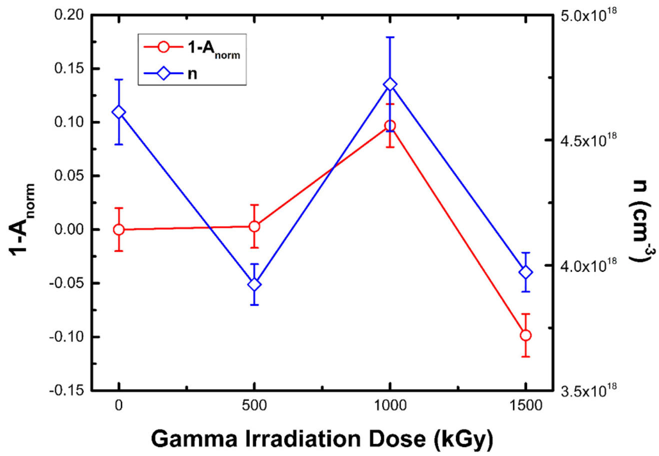

Fig. 6. Variations of total disorder ($1 - A_{norm}$) and free carrier concentration (n) of n-4H-SiC before and after gamma irradiation at different irradiation doses.

characteristics after exposed to certain gamma irradiation dose is also reported by various researchers [42,43]. The insignificant variation of $1 - A_{norm}$ after gamma irradiation doses demonstrates that the gamma-induced defect states are not greatly disturbing the n-4H-SiC crystal lattice.

To account for the role of defect states on the free carrier concentration (n), we also determined n from the Raman spectra by using an empirical relation deduced by Nakashima et al. [44]. The expression is given by

$$n = \Delta\omega^{1.0} \times 1.23 \times 10^{17}\mathrm{cm}^{-3} \tag{5}$$

where , $\omega_{LO} = 964.1\mathrm{cm}^{-1}$ for un-doped or semi-insulating 4H-SiC, ω_{LOPC} is the deconvoluted peak position at $1000\mathrm{cm}^{-1}$ as shown in Fig. 5. Therefore by evaluating the shift in the LOPC mode ($\Delta\omega$), n can be determined easily by using Eqn. (5). Fig. 6 shows the variation of n before and after gamma irradiation at different irradiation doses. As noticed, a clear evolution of n with irradiation dose was not observed in the present study. This indicating the existence of anomalies in the generation, modification and recombination of acceptor and donor type of defect states at both h- and k-sites of the n-4H-SiC crystal. At 500 kGy and 1500 kGy irradiation doses the decrease in n is mainly attributed to increase in the free electron capture by the acceptor type of defect states induced in the material. However as noticed from Fig. 6, the ratio of change in n at these irradiation doses to the unirradiated sample is less than $\sim$1.5%. On the other hand the increase in n at 1000 kGy with respect to the unirradiated sample is $\sim$0.25%. From the XRD studies it is also found that the maximum lattice distortion (change in $c/(n.\ a)$ ratio at 1000 kGy with respect to the unirradiated one) found to be less than 0.2% (supplementary figure). From these percentile values it can be easily established that the gamma-induced defect states are not significantly affecting on the bulk properties of n-4H-SiC.

However, the presence of defect states and/or n variation in the n-4H-SiC bulk would certainly influence the device characteristics (junction properties) of p-n diodes, Schottky diodes and MOSFETs. In the past the α-particle detection performance of the gamma-irradiated 6H-SiC based p-n diodes (Co-60 source, 1.17 and 1.33 MeV) [42] and 4H-SiC based Schottky diodes (Cs-137 source, 0.667 MeV) [45] have been reported. Based on the total dose effects, both the reports concluded on the radiation resistant property of SiC despite some modifications/anomalies observed in the leakage currents [42] or the detection performances at different irradiation doses [45]. And more recently some reports on the gamma-irradiated MOSFET structures (Co-60 source) showed a shift in the threshold voltage to the negative bias as well as increase in the leakage currents [43,46]. These observations are clearly indicating the influence of gamma-induced defect states in the 4H-SiC substrate on the device performance. In fact the observed leakage currents in the diodes and transistors are much anticipated takes place through the tunneling and/or trap-assisted tunneling mechanisms. On the other hand the decrease in the charge collection efficiency (CCE) of a detector to 84% after gamma irradiation [45] could be attributed for the free carrier capture by the acceptor type of defect states induced in the n-4H-SiC substrate. Similar radiation damage predictions could be approximated for the electron beam irradiation conducted at the energies close to that of Co-60 photons. But in view of the practical importance these effects are not significant compared to Si-based devices. Thus proving the radiation resistant property of 4H-SiC. However additional studies are required on the 4H-SiC substrate contribution to the devices which are exposed to energetic electrons and neutrons at elevated radiation doses.

4. Conclusion

The gamma irradiation effects on the structural and optical properties of n-4H-SiC were studied by using different characterization techniques. The gamma-induced lattice distortion ($c/(n.\ a)$ ratio) in the irradiated samples is ascribed to the distortion in the bonding tetrahedral of the crystal lattice by generating the various defect states. On an atomic scale this has led to anomalous variation in the c- and a- axis lattice constants of 4H-SiC. The Urbach energy (E_U), defect related photoluminescence bands (DPL bands) and LOPC modes are influenced by defect induced structural disorder in the material. Despite these effects, the overall gamma-induced disorder ($1 - A_{norm}$) and free carrier concentration (n) are not significant. Thus proving the radiation resistant property of n-4H-SiC.

Acknowledgments

This work has been carried out under UGC DAE CSR Indore, India collaborative research scheme (CSR-IC-BL-48/CRS-145-2014-15/1241). The authors would like to acknowledge Dr. M. T. Jose, Harikrishnan and Shailesh Joshi, RSD, IGCAR Kalpakkam for providing and carrying out gamma irradiation experiment. The authors would like to acknowledge Dr. Mukul Gupta, UGC DAE CSR Indore for providing XRD facility.

Appendix A. Supplementary data

Supplementary data to this article can be found online at https://doi.org/10.1016/j.nimb.2018.12.016.

References

[1] Tsunenobu Kimoto, James A. Cooper, Fundamentals of Silicon Carbide Technology: Growth, Wiley, Characterization, 2014.
[2] G.L. Harris, Properties of silicon carbide, Inspec (1995).
[3] G. Ferro, D. Chaussende, A new model for in situ nitrogen incorporation into 4H-SiC during epitaxy, Sci. Rep. 7 (2017) 1–11, https://doi.org/10.1038/srep43069.
[4] M. Ohkubo, S. Shiki, M. Ukibe, N. Matsubayashi, Y. Kitajima, S. Nagamachi, Nitrogen Dopants in SiC, 2012, pp. 1–5, , https://doi.org/10.1038/srep00831.
[5] F. Nava, G. Bertuccio, A. Cavallini, E. Vittone, Silicon carbide and its use as a radiation detector material, Meas. Sci. Technol. Meas. Sci. Technol. 19 (2008) 102001–102025, https://doi.org/10.1088/0957-0233/19/10/102001.
[6] L.Y. Liu, T.L. Shen, A. Liu, T. Zhang, S. Bai, S.R. Xu, P. Jin, Y. Hao, X.P. Ouyang, Performance degradation and defect characterization of Ni/4H-SiC Schottky diode neutron detector in high fluence rate neutron irradiation, Diam. Relat. Mater. 88 (2018) 256–261, https://doi.org/10.1016/j.diamond.2018.07.019.
[7] T. Egilsson, A. Henry, I.G. Ivanov, J.L. Lindström, E. Janzén, Photoluminescence of electron-irradiated 4H-SiC, Phys. Rev. B 59 (1999) 8008, https://doi.org/10.1103/PhysRevB.59.8008.
[8] H.J. Von Bardeleben, J.L. Cantin, Electron irradiation induced defects in monocrystalline 4H-SiC and 6H-SiC: the influence of the electron energy and doping, Appl. Surf. Sci. 184 (2001) 237–241, https://doi.org/10.1016/S0169-4332(01)00676-6.
[9] A. Le Donne, S. Binetti, S. Pizzini, Electrical and optical characterization of electron-irradiated 4H-SiC epitaxial layers annealed at low temperature, Diam. Relat. Mater. 14 (2005) 1150–1153, https://doi.org/10.1016/j.diamond.2004.10.020.

[10] A. Castaldini, A. Cavallini, L. Rigutti, F. Nava, S. Ferrero, F. Giorgis, Deep levels by proton and electron irradiation in 4H-SiC, J. Appl. Phys. 98 (2005), https://doi.org/10.1063/1.2014941.
[11] H.Y. Kim, J. Kim, J.A. Freitas, Penetration depth profiling of proton-irradiated 4H-SiC at 6 MeV and 8 MeV by micro-Raman spectroscopy, Appl. Surf. Sci. 270 (2013) 44–48, https://doi.org/10.1016/j.apsusc.2012.12.014.
[12] D.J. Brink, J.B. Malherbe, J. Camassel, Neutron irradiation effects in SiC, Nucl. Instrum. Meth. Phys. Res. Sect. B Beam Interact. Mater. Atoms 267 (2009) 2716–2718, https://doi.org/10.1016/j.nimb.2009.05.029.
[13] P.F. Wang, Y.F. Ruan, L. Huang, W. Zhu, Nitrogen-promoted formation of graphite-like aggregations in SiC during neutron irradiation, J. Appl. Phys. 111 (2012) 10–14, https://doi.org/10.1063/1.3697681.
[14] G. Litrico, M. Zimbone, L. Calcagno, P. Musumeci, G.A. Baratta, G. Fotil, Point defects induced in ion irradiated 4H–SiC probed by exciton lines, Nucl. Instrum. Meth. Phys. Res. Sect. B Beam Interact. Mater. Atoms 267 (2009) 1243–1246, https://doi.org/10.1016/j.nimb.2009.01.147.
[15] Chonghong Zhang, Yin Song, Yitao Yang, Chunlan Zhou, Long Wei, Hongji Ma, Evolution of defects in silicon carbide implanted with helium ions, Nucl. Instrum. Meth. Phys. Res. Sect. B Beam Interact. Mater. Atoms 326 (2014) 345–350, https://doi.org/10.1016/j.nimb.2013.10.064.
[16] R. Héliou, J.L. Brebner, S. Roorda, Optical and structural properties of 6H-SiC implanted with silicon as a function of implantation dose and temperature, Nucl. Instrum. Meth. Phys. Res. Sect. B Beam Interact. Mater. Atoms 175 (2001) 268–177273, https://doi.org/10.1016/S0168-583X(00)00633-9.
[17] S. Sorieul, J.-M. Costantini, L. Gosmain, G. Calas, J.-J. Grob, L. Thome, Study of damage in ion-irradiated α-SiC by optical spectroscopy, J. Phys.: Condens. Matter 18 (2006) 8493–8502.
[18] S. Sorieul, J.M. Costantini, L. Gosmain, L. Thomé, J.J. Grob, Raman spectroscopy study of heavy-ion-irradiated α-SiC, J. Phys. Condens. Matter. 18 (2006) 5235–5251, https://doi.org/10.1088/0953-8984/18/22/022.
[19] S. Sorieul, X. Kerbiriou, J.-M. Costantini, L. Gosmain, G. Calas, C. Trautmann, Optical spectroscopy study of damage induced in 4H-SiC by swift heavy ion irradiation, J. Phys. Condens. Matter. 24 (2012) 125801, , https://doi.org/10.1088/0953-8984/24/12/125801.
[20] Indudhar Panduranga Vali, Pramoda Kumara Shetty, M.G. Mahesha, Rashmitha Keshav, V.G. Sathe, D.M. Phase, R.J. Choudhary, Gamma irradiation effects on Al/n-Si Schottky junction properties, Nucl. Instrum. Meth. Phys. Res. Sect. B Beam Interact. Mater. Atoms. 436 (2018) 191–197.
[21] M. Kanaya, J. Takahashi, Y. Fu18jiwara, A. Moritani, Controlled sublimation growth of single crystalline 4H-SiC and 6H-SiC and identification of polytypes by x-ray diffraction, Appl. Phys. Lett. 58 (1991) 56–58, https://doi.org/10.1063/1.104443.
[22] Z.C. Feng, A. Rohatgi, C.C. Tin, R. Hu, Structural, optical, and surface science studies of 4H-SiC epilayers grown by low pressure chemical vapor deposition, J. Electron. Mater. 25 (1996) 917–923.
[23] Y. Cui, X. Hu, K. Yang, X. Yang, X. Xie, L. Xiao, X. Xu, Influence of nitrogen concentrations on the lattice constants and resistivities of n-Type 4H-sic single crystals, Cryst. Growth Des. 15 (2015) 3131–3136, https://doi.org/10.1021/cg501216d.
[24] S. Limpijumnong, W. Lambrecht, S. Rashkeev, B. Segall, Optical-absorption bands in the 1–3 eV range in n-type SiC polytypes, Phys. Rev. B 59 (1999) 12890–12899, https://doi.org/10.1103/PhysRevB.59.12890.
[25] P.J. Wellmann, S. Bushevoy, R. Weingärtner, Evaluation of n-type doping of 4H-SiC and n-/p-type doping of 6H-SiC using absorption measurements, Mater. Sci. Eng. B Solid-State Mater. Adv. Technol. 80 (2001) 352–356, https://doi.org/10.1016/S0921-5107(00)00598-5.
[26] E. Biedermann, The optical absorption bands and their anisotropy in the various modifications of SiC, Solid State Commun. 3 (1965) 343–346, https://doi.org/10.1016/0038-1098(65)90092-X.
[27] J. Tauc, Amorphous and Liquid Semiconductors, Plenum, London, 1974, p. 170.
[28] N.F. Mott, E.A. Davis, Electronic Processes in Non-Crystalline Materials, 2nd ed., Oxford, Clarendon, 1979.
[29] A. Lohrmann, B.C. Johnson, J.C. McCallum, S. Castelletto, A review on single photon sources in silicon carbide, Reports Prog. Phys. 80 (2017), https://doi.org/10.1088/1361-6633/aa5171.
[30] T.A. Eberlein, C.J. Fall, R. Jones, P.R. Briddon, S. Öberg, Alphabet luminescence lines in 4H-Sic, Phys. Rev. B – Condens. Matter Mater. Phys. 65 (2002) 1841081–1841084, https://doi.org/10.1103/PhysRevB.65.184108.
[31] L. Storasta, F.H.C. Carlsson, S.G. Sridhara, J.P. Bergman, A. Henry, T. Egilsson, A. Hallén, E. Janzén, Pseudodonor nature of the D1 defect in 4H-SiC, Appl. Phys. Lett. 78 (2001) 46–48, https://doi.org/10.1063/1.1334907.
[32] S.I. Maximenko, J.A. Freitas, N.Y. Garces, E.R. Glaser, M.A Fanton, Evolution of D1-defect center in 4H-SiC during high temperature annealing, Mater. Sci. Forum 600–603 (2009) 429–432, https://doi.org/10.4028/www.scientific.net/MSF.600-603.429.
[33] W. Sullivan, J.W. Steeds, A study of the D II defect after electron irradiation and annealing of 4H SiC, Mater. Sci. Forum 557 (2007) 319–322, https://doi.org/10.4028/www.scientific.net/MSF.556-557.319.
[34] Chao Jiang, Dane Morgan, Izabela Szlufarska, Carbon tri-interstitial defect: a model for the DII center, Phys. Rev. B 86 (2012) 144118, , https://doi.org/10.1103/PhysRevB.86.144118.
[35] L. Torpo, S. Pöykkö, R. Nieminen, Antisites in silicon carbide, Phys. Rev. B – Condens. Matter Mater. Phys. 57 (1998) 6243–6246, https://doi.org/10.1103/PhysRevB.57.6243.
[36] A.A. Lebedev, B.Y. Ber, N.V. Seredova, D.Y. Kazantsev, V.V. Kozlovski, Radiation-stimulated photoluminescence in electron irradiated 4H-SiC, J. Phys. D. Appl. Phys. 48 (2015) 485106, , https://doi.org/10.1088/0022-3727/48/48/485106.
[37] J.W. Steeds, W. Sullivan, A. Wotherspoon, J.M. Hayes, Long-range migration of intrinsic defects during irradiation or implantation, J. Phys. Condens. Matter. 21 (2009), https://doi.org/10.1088/0953-8984/21/36/364219.
[38] S. Nakashima, H. Harima, Raman investigation of SiC polytypes, Phys. Status Solidi Appl. Res. 162 (1997) 39–64, https://doi.org/10.1002/1521-396X(199707)162:1 < 39::AID-PSSA39 > 3.0.CO; 2-L.
[39] M. Bauer, A.M. Gigler, A.J. Huber, R. Hillenbrand, R.W. Stark, Temperature-depending Raman line-shift of silicon carbide, J. Raman Spectrosc. 40 (2009) 1867–1874, https://doi.org/10.1002/jrs.2334.
[40] H. Harima, S.I. Ntsuakashima, T. Uemura, Raman scattering from anisotropic LO-phonon-plasmon-coupled mode in n-type 4H- and 6H-SiC, J. Appl. Phys. 78 (1995) 1996–2005, https://doi.org/10.1063/1.360174.
[41] R. Menzel, K. Gärtner, W. Wesch, H. Hobert, Damage production in semiconductor materials by a focused Ga + ion beam, J. Appl. Phys. 88 (2000) 5658–5661, https://doi.org/10.1063/1.1319168.
[42] Akimasa Kinoshita, Motohiro Iwami, Ken-ichi Kobayashi, Itsuo Nakano, Reisaburo Tanaka, Tomihiro Kamiya, Akihiko Ohi, Takeshi Ohshima, Yasutaka Fukushima, Radiation effect on pn-SiC diode as a detector, Nucl. Instrum. Meth. Phys. Res. A 541 (2005) 213–220.
[43] Takuma Matsuda, Takashi Yokoseki, Satoshi Mitomo, Koichi Murata, Takahiro Makino, Hiroshi Abe, Akinori Takeyama, Shinobu Onoda, Yuki Tanaka, Mikio Kandori, Toru Yoshie, Yasuto Hijikata, Takeshi Ohshima, Change in characteristics of SiC MOSFETs by gamma-ray irradiation at high temperature, Mater. Sci. Forum 858 (2015) 860–863, https://doi.org/10.4028/www.scientific.net/MSF.858.860.
[44] S. Nakashima, T. Kitamura, T. Kato, K. Kojima, R. Kosugi, H. Okumura, H. Tsuchida, M. Ito, Determination of free carrier density in the low doping regime of 4H-SiC by Raman scattering, Appl. Phys. Lett. 93 (2008) 121913.
[45] Frank H. Ruddy, John G. Seidel, The effects of intense gamma-irradiation on the alpha-particle response of silicon carbide semiconductor radiation detectors, Nucl. Instrum. Meth. Phys. Res. Sect. B Beam Interact. Mater. Atoms 263 (2007) 163–168.
[46] Takeshi Ohshima, Takashi Yokoseki, Koichi Murata, Takuma Matsuda, Satoshi Mitomo, Hiroshi Abe, Takahiro Makino, Shinobu Onoda, Yasuto Hijikata, Yuki Tanaka, Mikio Kandori, Shuichi Okubo, Toru Yoshie, Radiation response of silicon carbide metal–oxide–semiconductor transistors in high dose region, Jpn. J. Appl. Phys. 55 (2016) 01AD01.